Mechanical Membrane Injury Induces Axonal Beading through Localized Activation of Calpain

Devrim Kilinc, Ph.D.,
School of Biomedical Engineering, Science, and Health Systems, Drexel University, Philadelphia, Pennsylvania 19104 USA. Current address: Université Pierre & Marie Curie, Laboratoire de Neurobiologie des Processus Adaptatifs, Paris, France

Gianluca Gallo, Ph.D., and
Department of Neurobiology and Anatomy, Drexel University College of Medicine, Philadelphia, Pennsylvania 19129 USA

Kenneth A. Barbee, Ph.D.
School of Biomedical Engineering, Science, and Health Systems, Drexel University, Philadelphia, Pennsylvania 19104 USA

Abstract

Diffuse axonal injury (DAI), a major component of traumatic brain injury, is characterized by a sequence of neurochemical reactions initiated at the time of trauma and resulting in axonal degeneration and cell death. Calcium influx through mechanically induced axolemmal pores and subsequent activation of calpains are thought to be responsible for the cytoskeletal damage leading to impaired axonal transport. Focal disruption of cytoskeleton accompanied by the accumulation of transported membranous cargo leads to axonal beading which is the characteristic morphology of DAI. By applying fluid shear stress injury on cultured primary neurons, acute calcium (Ca^{2+}) and calpain responses of axons to mechanical trauma were investigated. Intracellular Ca^{2+} concentration ($[Ca^{2+}]_i$) shows a steady increase following injury that can be blocked by sealing membrane pores with Poloxamer 188 and by chelating intra- or extracellular Ca^{2+}. Calpain activity increases in response to mechanical injury and this increase depends on Ca^{2+} availability and on axolemmal permeability. Both the $[Ca^{2+}]_i$ increase and calpain activity exhibit focal peaks along the axons which co-localize with mitochondria and predict future axonal bead locations. These findings suggest that mechanoporation may be the initiating mechanism resulting in ensuing calcium fluxes and subsequent calpain activity and that post-injury membrane repair may be a valid therapeutic approach for acute intervention in DAI.

Keywords

Address for manuscript correspondence: School of Biomedical Engineering, Science, and Health Systems, Drexel University, 3141 Chestnut St., Philadelphia, Pennsylvania 19104 USA. Tel: +1 215 895 1335 Fax: +1 215 895 4983. barbee@drexel.edu (K.A. Barbee).

INTRODUCTION

Traumatic brain injury (TBI) is a major cause of disability and death worldwide; from 100 to 350 patients per 100,000 inhabitants are admitted to hospital care following a TBI, of which approximately 80% are mild injuries (Servadei et al., 2007). More than 11.5 million people are estimated to live with TBI-related disability, impairment, complaint or handicap in Europe and the USA alone (Schouten, 2007). Yet with this enormous burden to the society, there is no clinically proven therapy available to limit the neuropathological sequelae of TBI (Wang et al., 2006). The diffuse form of TBI, diffuse axonal injury (DAI), is associated with the inertial forces applied to the head at the time of the injury. The resulting large deformations of the brain tissue does not immediately sever axons (Gennarelli et al., 1998; Maxwell et al., 1993), but microstructural cellular damage leads to a spectrum of neurochemical changes (McIntosh et al., 1996) that can result in axonal bead formation leading to disconnection from target tissues and cell death (Gaetz, 2004; Raghupathi, 2004). Understanding the neurobiological mechanisms of the post-traumatic sequelae of events will enable identifying potential therapeutic targets for clinical intervention.

Mechanoporation, the generation of transient membrane pores due to mechanical tissue deformation has been suggested to underlie DAI (Buki and Povlishock, 2006; Gennarelli, 1996). Calcium ions (Ca^{2+}) entering the cytoplasm due to the steep concentration gradient across the membrane could initiate a series of cascade reactions that eventually lead to the degeneration of the axon and secondary neuronal cell death (Gaetz, 2004). Activation of calpains, Ca^{2+}-activated neutral proteases, due to high intracellular Ca^{2+} concentration ($[Ca^{2+}]_i$) is a key event in the DAI pathology (Liu et al., 2008). Calpains are known to degrade cytoskeletal proteins such as microtubule-associated proteins, spectrin, and tubulin (Billger et al., 1988; Johnson et al., 1991); however there is no direct evidence of degradation of microtubules by calpains. Loss of microtubules among other cytoskeletal proteins leads to impaired axonal transport resulting in axonal beading morphology (Maxwell and Graham, 1997) as microtubules are mainly responsible for motor-based axonal transport (Coleman, 2005). It has been recently shown by our group that shear stress injury on cultured neurons causes mechanoporation-induced focal disruption of axonal microtubules and subsequent axonal beading (Kilinc et al., 2008).

$[Ca^{2+}]$ has been shown to increase within 1 hour (h) following *in vivo* TBI in a variety of experimental models (Fineman et al., 1993; Maxwell et al., 1995; Shapira et al., 1989). *In vitro*, a sharp increase in $[Ca^{2+}]_i$ was observed immediately following injury; however, the maintenance of $[Ca^{2+}]_i$ seems to depend on the type of injury. A sudden drop in $[Ca^{2+}]_i$ to basal levels within 2 min was observed following biaxial stretch injury (Cargill and Thibault, 1996), whereas a slow decrease in $[Ca^{2+}]_i$ was observed following fluid shear stress injury (LaPlaca et al., 1997). Following uniaxial stretch injury, a gradual increase for at least 1h was observed and was due to the early proteolysis of the a-subunit of the tetrodotoxin-sensitive voltage gated Na^+ channels (Iwata et al., 2004; Wolf et al., 2001). Recently, Ca^{2+}-permeable AMPA receptors following *in vitro* stretch injury were shown to be critical in the Ca^{2+} influx (Spaethling et al., 2008). These results show that the time course and the pathway of the Ca^{2+} influx highly depends on the injury type and needs further clarification for establishing a causal link between $[Ca^{2+}]_i$ rise and subsequent neuropathology.

In head injured humans, activated μ-calpain and calpain-mediated spectrin breakdown products were shown to increase compared to control levels (McCracken et al., 1999). Calpains were shown to be active and functional as early as 15 min following *in vivo* TBI (Kampfl et al., 1996) and calpain-mediated spectrin breakdown was detected in the brain areas associated with high cell death at 90 min post-injury (Saatman et al., 1996). Calpain activation has been shown to follow a biphasic pattern following injury as demonstrated by acute and delayed decreases

in cytoskeletal proteins (Saatman et al., 2003; Serbest et al., 2007). Early activation of calpain is suggested to contribute in the progressive structural damage in the axonal cytoskeleton following injury whereas the delayed activation is attributed to the late phases of axonal degeneration (Saatman et al., 2003). Although the hypothesis suggesting that early activation of calpains due to Ca^{2+} influx through mechanoporated plasma membrane seems reasonable, a recent study showed that calpain-mediated spectrin breakdown was detected in a small fraction of mechanoporated axons but in a larger fraction of the axons which showed delayed membrane perturbation, probably associated with later stages of neurodegeneration (Farkas et al., 2006). The temporal and spatial activation and activity pattern of calpain following mechanical trauma are currently unknown.

Poloxamer 188 (P188) is a nontoxic, nonionic, tri-block amphiphilic co-polymer (MW: ~8400) consisting of a central hydrophobic polyoxypropylene molecule that is flanked on both sides by two hydrophilic chains of polyoxyethylene. P188 has been shown to be capable of sealing damaged cell membranes (Maskarinec et al., 2005) suggesting a novel pharmacological strategy against cell injury. Electroporated (Lee et al., 1992), irradiated (Greenebaum et al., 2004), and thermally damaged (Padanilam et al., 1994) skeletal muscle cell membranes were shown to be resealed by P188. In primary neuron culture, P188 was shown to save neurons from excitotoxic or oxidative stress-related necrosis and from electroporation (Marks et al., 2001). The ability of P188 to protect neuronal cells from trauma-induced necrotic and apoptotic death via membrane repair was previously demonstrated (Serbest et al., 2005; Serbest et al., 2006). It was recently shown by our group that P188 blocks mechanically-induced increase in membrane permeability and subsequent cytoskeletal disruption and transport impairment in cultured primary neurons (Kilinc et al., 2008). *In vivo*, post-injury delivery of P188 was able to protect neurons following spinal cord compression injury (Borgens et al., 2004), excitotoxic injury (Curry et al., 2004; Frim et al., 2004) and acute intraparenchymal brain hemorrhage (Cadichon et al., 2007). Collectively, these studies show the ability of P188 to repair damaged cell membranes and to rescue neurons following a variety of insults. However, it is not known if the neuroprotective effect of P188 is via blocking the post-traumatic increase in $[Ca^{2+}]_i$ and subsequent calpain activity.

Using an *in vitro* model of mechanical injury, it has recently been demonstrated that mechanoporation leads to focal microtubule disruption, organelle accumulation and subsequent focal axonal beading leading to degeneration of the axon (Kilinc et al., 2008). In the current paper, the initial Ca^{2+} and calpain response of the axons to mechanical injury was examined. In contrast with previous reports (Cargill and Thibault, 1996; Geddes-Klein et al., 2006a; Geddes-Klein et al., 2006b; LaPlaca et al., 1997; Lusardi et al., 2004; Spaethling et al., 2008; Wolf et al., 2001), $[Ca^{2+}]$ exhibits a steady increase that depends on intra- and extracellular Ca^{2+} and that can be blocked by sealing membrane pores. Similarly, calpain activity is higher in the injured neurons and is regulated by Ca^{2+} influx through mechanically induced poration. Both $[Ca^{2+}]$ increase and calpain activity have focal peaks at distinct locations along the axons that co-localize with axonal mitochondria and constitute future axonal beads. These observations suggest the mitochondrion as a key player in the injury-induced $[Ca^{2+}]_i$ increase and calpain activation.

MATERIALS AND METHODS

Cell Culture and Reagent

Embryonic day 8 chick forebrain neurons were harvested, dissociated and plated on German glass coverslips (Bellco Glass, Vineland, NJ) at a concentration of 1.5×10^4 cells·cm^{-2} (Heidemann et al., 2003). Chick forebrain neurons are very similar to cultured mammalian hippocampal neurons and are commonly used as a cell model system to study axonal neurobiology (Heidemann et al., 2003). In experiments requiring tracking of multiple neurons,

indexed coverslips (Bellco) were used to track individual neurons. Coverslips were treated with 2-[2-(3-Trimethoxy-silyl-propyl-amino)-ethylamino]-ethylamine (Sigma, St. Louis, MO) to promote attachment as described elsewhere (Geddes et al., 2003). Cultures were maintained in supplemented M199 medium (Invitrogen, Carlsbad, CA) and incubated (5% CO_2; 37°C) for 4–6 days before experimentation. Culture medium was changed every other day. HEPES buffered, supplemented Ham's F12 medium (Invitrogen) was used as experimental medium during live imaging experiments.

Experimental Procedure

The controlled shear stress device is based on a cone-and-plate viscometer and applies uniform shear stress over the coverslip area through the controlled rotation of the cone (Blackman et al., 2000). When used with high onset rates the rotation of the cone, which is in fluidic contact with the cell culture, induces fluid shear stress injury in neurons (Kilinc et al., 2008). A shear impulse of 45dyn·cm^{-2} with 20 ms onset time was consistently used to induce shear stress injury. Sham (uninjured) controls underwent the exact protocol except without the cone rotation. A stage heater (NevTek, Burnsville, VA) maintained constant temperature (37°C) during experiments. Images were taken with an inverted Nikon Diaphot Eclipse TE300 microscope (Optical Apparatus, West Chester, PA). In experiments testing the effect of P188 treatment, P188 (Pluronic acid F-68, Sigma) was dissolved in the experimental medium and applied to neurons 5 min post-injury with a final concentration of 100μM.

Beading Analysis

Indexed coverslips allow tracing of individual neurons during the experiment, enabling us to image 7–8 neurons per coverslip. Images were obtained immediately after and 60–90 min after the injury. To quantify axonal beading, we used a Matlab-based (MathWorks, Natick, MA) interactive image analysis program that successfully detects axonal beading(Kilinc et al., 2009). The beading score is the volume-weighted sum of the radii of axonal swellings, whose diameter was at least twice the axon diameter, normalized by the length of the axon in question. Change in the beading score, normalized by the time period between two image acquisitions, was calculated for each individual axon and compared among different experimental groups.

[Ca^{2+}]$_i$ Measurement and Quantification

Fluo-3 was used as the Ca^{2+} indicator. When compared with Fura-2, the higher dissociation constant (K_d) value (0.325 vs. 0.14μM) reduces the buffering of the [Ca^{2+}]$_i$ signal. In addition, the longer excitation wavelength avoids the cell damage by exposure to UV, and its large optical signal provides very good signal-to-noise ratio (Merritt et al., 1990). To control for the effect of volume changes on the fluorescence intensity, Fluo-3 was used in tandem with the volumetric intracellular marker, CellTracker Red (CTR, Invitrogen). Prior to experiment, neurons were incubated in the dark with experimental medium containing 3.3 μM CTR and 5μM Fluo-3 for 20 min and rinsed twice with experimental medium. Up to three predetermined areas on the coverslip were imaged before and after the injury, with 5 min intervals using appropriate filter sets for the two indicators. Image acquisition settings were kept constant among different experimental groups. To avoid photo-bleaching, locating the neurons and focusing were conducted under red fluorescence, as CTR was brighter and more bleach-resistant than Fluo-3. The ratio of background-subtracted average intensities of Fluo-3 over CTR at the axonal area (excluding focal peaks) was analyzed over time to compare [Ca^{2+}]$_i$ rise among different experimental groups. Similarly, the average intensities at the bright spots were used to calculate the ratio. For intracellular Ca^{2+} chelation, 20 μM 1,2-Bis(2-aminophenoxy) ethane-N,N,N′,N′-tetraacetic acid tetrakis-AM (BAPTA-AM, Invitrogen) was added to the incubation medium (along with Fluo-3 and CTR). For extracellular Ca^{2+} chelation, the

experimental medium was buffered with 1 mM ethyleneglycol-O, O′-bis(2-aminoethyl)-N, N, N′, N′-tetraacetic acid (EGTA, Sigma).

Calpain Measurement and Quantification

To detect calpain activity in living neurons, the fluorogenic calpain substrate 7-amino-4-chloromethylcoumarin, *t*-BOC-L-leucyl-L-methionine amide (t-BOC; Invitrogen) was used. Non-fluorescent t-BOC freely diffuses into the cell and becomes membrane-impermeant after being conjugated to a thiol. Cleavage of t-BOC-thiol by calpain results in the release of fluorescent 7-amino-4-methylcoumarin-thiol (MAC-thiol). The formation of MAC-thiol is not reversible. Therefore, steady state calpain activity level results in an increase in fluorescence due to the accumulation of MAC-thiol. Changes in calpain activity can thus be detected by considering the rate of change in the MAC-thiol fluorescent signal (Rosser et al., 1993). Prior to experiment, neurons were incubated with experimental medium containing 5μM CTR and rinsed twice with experimental medium. Rinsing was followed by incubation with the experimental medium containing 10μM t-BOC for 10–15 min. Neurons were injured as described above, and a fixed area on the coverslip was imaged at 5 min intervals for 20–25 min post-injury. An excitation/emission filter set suitable for DAPI was used to record t-BOC fluorescence. Since t-BOC demonstrated photo-activation as well as photo-toxicity, exposure to ultraviolet light was kept minimal, using CTR signal to control focal plane. In experimental groups involving Calpain inhibition, neurons were incubated and experimented in media containing 3μM Calpain Inhibitor I or N-Acetyl-Leu-Leu-Nle-CHO (ALLN; Calbiochem). The percent change in the rate of t-BOC signal intensity vs. time was calculated for individual axons and used in comparison among different experimental groups.

Staining of Mitochondria

Neurons were stained with mitochondrion specific MitoTracker-Green dye (Invitrogen) to investigate distribution of axonal mitochondria relative to focal CTR peaks and phase contrast images of the axon. Neurons were exposed to 5 nM MitoTracker for 60 min before simultaneous phase contrast and fluorescent imaging.

Statistical Analysis

In axonal beading measurements, we analyzed 5–9 neurons per coverslip and used 3–8 coverslips per experimental condition. N for statistical calculations is the number of axons. Data were expressed as mean ± 90% confidence intervals. Statistical analysis was performed using one way analysis of variance (ANOVA), followed by Tukey-Kramer's *post hoc* test to determine one-tail p values between different experimental groups.

RESULTS

Axonal Beading Requires Calcium and Calpain Activity

Fluid shear stress injury was applied to chick forebrain neurons at 4–6 days *in vitro*. To determine the roles of extra- and intracellular Ca^{2+} in the post-injury beading response, neurons were injured in the experimental medium buffered with 1 mM EGTA or pre-incubated with 20 μM BAPTA prior to injury, respectively. To determine the effect of the calpain inhibition on axonal beading, neurons were incubated with 3 μM ALLN prior to and after the injury. Figure 1A shows a representative neuron pre- and 30–60 min, where axonal beading morphology is presented. Axonal beading is reduced to the levels of sham controls by chelating intra- and extracellular Ca^{2+} and by directly inhibiting calpain activity in the absence of calcium chelators (Figure 1B).

Injury-induced Increase in Axonal $[Ca^{2+}]_i$ Is Inhibited by Ca^{2+} Chelators and by P188

Calcium imaging was performed using Fluo-3 loaded neurons. The calcium signal was normalized by taking the ratio of the Fluo-3 signal to that of CellTracker Red (CTR), a fluorescent cytoplasmic reporter. Neurons were subjected to injury and imaged for 20–30 min taking a snapshot every 5–10 min. Figure 2A shows a sham control and an injured neuron over the course of 30 min post-injury. In the sham controls the average of Fluo-3/CTR signal intensity ratio is steady for the axonal area as well as for focal $[Ca^{2+}]_i$ peaks. In the injured neurons, the axonal average of the intensity ratio shows a gradual increase. At the focal peaks, the increase has a higher initial rate compared to the rest of the axon but decreases back to the levels of the axon average by 20 min post-injury time point (Figure 2B). The rate of change in the Fluo-3/CTR signal ratio in axonal areas and in focal peaks is significantly higher in the injury group when compared to sham controls at all post-injury time points. EGTA, BAPTA and P188 effectively block the increase in the rate of change (Figure 2C). Collectively, these results show that injury-induced $[Ca^{2+}]_i$ rise depends on the availability of extracellular Ca^{2+}, existence of membrane pores and the status of the intracellular Ca^{2+} buffering system.

Injury-induced Increase in the Calpain Activity Is Regulated by Membrane Permeability and Ca^{2+} Availability

t-BOC is a fluorogenic reporter of calpain activity which freely diffuses into the cell and fluoresces when specifically cleaved by calpain (Robles et al., 2003). Following the addition of t-BOC to the culture medium the fluorescence level increases steadily due to the calpain activity in the cell. Changes in calpain activity can thus be detected by considering the rate of change in the fluorescence signal. Post-injury calpain activity in the neurons was measured by the rate of change in the t-BOC fluorescence over time. In the sham controls, baseline calpain activity was detected as a slow increase in the t-BOC signal due to the retention of the fluorescent cleaved t-BOC molecule in the cytoplasm. When the neuron is injured, this increase in the signal is more pronounced (Figure 3A). As in the case of $[Ca^{2+}]_i$, there exist focal t-BOC peaks that correspond to axonal regions showing higher CTR and t-BOC signal intensity. Injured axons have higher calpain activity compared to sham controls, and in both sham control and injury groups there are focal peaks of calpain activity, where the t-BOC signal is higher than the rest of the axon (Figure 3B). For each axon and focal peak, the slope of the t-BOC signal vs. time curve is considered as one data point indicating calpain activity. The calpain activity in the sham controls was not different than the incubator controls (cells treated identically except not placed in the injury device), and ALLN reduced the rate of basal calpain activity significantly. Shear stress injury induced an increase in the calpain activity that could be blocked by ALLN, BAPTA, EGTA, and post-injury P188 treatment both in the axon and in focal peaks of calpain activity (Figures 3C and 3D). These findings indicate that post-injury calpain activity depends on extracellular and intracellular Ca^{2+} availability and can be inhibited by sealing membrane pores with P188.

Focal Peaks of Calpain Activity Co-localize with Mitochondria and Predict Bead Formation Sites

Focal peaks of CTR concentration were observed to occur normally in healthy neuron cultures. Shear stress injury was applied to CTR-loaded neurons, and they were tracked over the post-injury period to investigate the localization of these focal CTR peaks relative to injury-induced axonal beads (Figure 4A). 81.5% of all post-injury beads detected at 2h post-injury (N = 22 neurons) were co-localized with pre-injury focal CTR peaks, which lacked any sign of beading before the injury. Likewise, 67.7% of pre-injury focal CTR peaks predicted future bead locations. The distribution and size of focal CTR peaks were similar to those of axonal mitochondria. Therefore, in order to establish a relationship between focal CTR peaks with mitochondria, mitochondria and cytoplasm were simultaneously stained with MitoTracker

Green and with CTR, respectively (Figure 4B). 84.0% of all focal CTR peaks analyzed were associated with mitochondria (n = 119 peaks). These findings indicate that axonal beads develop at those locations where mitochondria are localized. As mitochondria are known to play a major role in intracellular Ca^{2+} dynamics (Wang et al., 2003), this co-localization suggests that axonal beads preferentially occur at those spots where a sustained disturbance in the ionic balance is evident. Furthermore, these same spots were shown to exhibit sharper $[Ca^{2+}]_i$ increases and higher calpain activity compared to the rest of the axon.

DISCUSSION

Fluid shear stress injury was applied to cultured primary neurons and post-injury $[Ca^{2+}]_i$ and calpain activity was observed. Ca^{2+}-dependent calpain activity was found to underlie post-injury axonal beading. Intracellular and extracellular Ca^{2+} chelation and calpain inhibition reduced injury-induced axonal beading to the levels of uninjured controls. Increase in $[Ca^{2+}]_i$ and calpain activity following mechanical injury was blocked by chelating intracellular or extracellular Ca^{2+} and by repairing the cell membrane with Poloxamer 188 (P188). $[Ca^{2+}]$ and calpain signals were heterogeneous along the axons and demonstrated focal peaks which corresponded to the locations of axonal mitochondria. The majority of these focal spots became axonal beads later in the injury progression, suggesting a causal relationship between Ca^{2+}, calpain dynamics, and the formation of axonal beads. The apparent association between mitochondria and bead formation is intriguing, and further studies are required to elucidate the role of mitochondria in calcium dynamics and subsequent pathology in injured axons.

Calcium rise and subsequent calpain activity play important roles in injury-induced neuropathology following TBI. Understanding the spatial and temporal patterns of axonal calcium concentration and calpain activity will shed light on the mechanisms of mechanoporation-induced axonal beading (Blumbergs et al., 1995; Strich, 1961). It is hypothesized that mechanoporation-induced rise in the $[Ca^{2+}]_i$ activates calpains (Liu et al., 2008) which would then cause disruption of the axonal cytoskeleton, specifically microtubules, which are the main conduits for axonal transport (Coleman, 2005). Focal disruptions of microtubules would lead to axonal transport impairment and subsequent accumulation of transported cargo consisting of proteins and vesicle-bound organelles such as mitochondria. According to this hypothesis, influx of extracellular Ca^{2+} is the initiating event of the post-traumatic proteolytic activity and subsequent axonal beading. Here, it is demonstrated that the influx of extracellular Ca^{2+} is indeed necessary for the increase in $[Ca^{2+}]_i$, increase in calpain activity and axonal bead formation following *in vitro* mechanical injury. The finding that intracellular chelation of Ca^{2+} by pre-injury loading of BAPTA inhibits $[Ca^{2+}]_i$ rise, calpain activity, and axonal beading suggests that the state of the intracellular Ca^{2+} buffering is also important in the effectiveness of Ca^{2+} influx. The presence of BAPTA would increase the Ca^{2+} buffering capacity in the axons and thereby block the increase in $[Ca^{2+}]_i$. It is also demonstrated that calpain activity is an essential step for axonal bead formation by showing that beading is blocked by the specific inhibition of calpains. Taken together, these observations support the suggested mechanism for the mechanically-induced neuronal degeneration where calpain-mediated disruption of microtubules and subsequent impairment of axonal transport lead to axonal beading. Since Ca^{2+} and calpain activity are shown to be crucial for axonal degeneration, inhibition of initial $[Ca^{2+}]_i$ increase via resealing mechanically-induced membrane pores may have a therapeutic potential following TBI.

Direct measurements of $[Ca^{2+}]_i$ and calpain activity following mechanical injury provides further information on the subcellular localization and dynamics of these key elements. In contrast to previous studies (Cargill and Thibault, 1996; Geddes-Klein et al., 2006a; Geddes-Klein et al., 2006b; LaPlaca et al., 1997; Lusardi et al., 2004; Spaethling et al., 2008; Wolf et al., 2001) an immediate, sharp $[Ca^{2+}]_i$ increase following injury was not observed. The

explanation for not observing a sharp increase in $[Ca^{2+}]_i$ may be the unique combination of the application of shear stress injury and the use of cultured primary neurons in this model. Also, previous studies report somatic or total $[Ca^{2+}]_i$ signal, rather than focusing on the axonal Ca^{2+}. In the literature, steady post-injury increase of $[Ca^{2+}]_i$ was indeed demonstrated in different experimental settings. *In vitro*, axonal stretch injury-induced a steady increase in the $[Ca^{2+}]_i$ following brief, sharp peak in the signal (Wolf et al., 2001). *In vivo*, a recent study demonstrated long lasting (up to 7 days) increase in basal $[Ca^{2+}]_i$ following brain injury (Sun et al., 2008).

The occurrence of focal axonal $[Ca^{2+}]_i$ peaks in a traumatic injury model is demonstrated for the first time. It is also remarkable that these peaks were associated with pre-injury mitochondria locations and underlie the morphological pattern of axonal bead formation. The dynamic intracellular Ca^{2+} mechanisms responsible for the initiation and the maintenance of these focal ion gradients should be studied in depth in order to enhance the understanding on the focal events in early and late phases of axonal pathology. Due to diffusion, the existence of focal gradients is only possible by sustained Ca^{2+} flux to that region. As these regions co-localize with mitochondria, one would suspect Ca^{2+} release from these organelles in the early post-injury period. Mitochondrial dysfunction follows acute brain injury due to the loss of intracellular ion balance and increase in $[Ca^{2+}]_i$ (Merenda and Bullock, 2006). Mitochondrial dysfunction has been demonstrated in *in vivo* TBI, where resulting Ca^{2+} accumulates in the organelle and cellular energy is lost (Xiong et al., 1997; Zhou et al., 2007). The relationship between the localization of mitochondria and the sites of beading is interesting and suggests the possibility that mitochondria may contribute, through their regulation of calcium levels, to axonal beading. However, future work will have to address the role of mitochondria in the formation of axonal beads.

In vivo calpain activity has been observed as early as 15 min post-injury (Kampfl et al., 1996) and was shown to exhibit a biphasic pattern where early activation was suggested to contribute in the progressive structural damage in the axonal cytoskeleton whereas the delayed activation was attributed to the late phases of axonal degeneration (Saatman et al., 2003). Calpain-mediated spectrin breakdown following traumatic injury was observed in a variety of experimental settings (Buki et al., 1999; Kampfl et al., 1996; McCracken et al., 1999; Saatman et al., 1996); however, injury-induced calpain activity has not been directly monitored. Using an established protocol for the detection of calpain activity in neurons (Robles et al., 2003), this study demonstrates the early activity of calpain observed in injury models *in vivo* (Kampfl et al., 1996; Saatman et al., 2003) and monitors the activity pattern of axonal calpain. The locations that exhibited focal peaks of $[Ca^{2+}]_i$ also exhibited higher calpain activity compared to the rest of the axon. There is approximately three times more calpain activity at these focal peaks compared to the rest of the axon suggesting that focal calpain activity is causing focal disruption of microtubules, as previously reported by our group (Kilinc et al., 2008). Local concentration of calpain-mediated spectrin breakdown products have been observed around dilated mitochondria in the somata of traumatically injured rat brain, suggesting a link between mitochondria and focal calpain activity (Farkas et al., 2006). Further studies are necessary to explain how focal Ca^{2+} and calpain peaks are initiated and maintained in the axons.

The full mechanistic roles of calcium in the beading response remain to be elucidated. Since calcium elevations contribute to membrane resealing through calcium-dependent proteins (Detrait et al., 2000; Yoo et al., 2003), it seems unlikely that this role of calcium would contribute negatively to the development of axonal injury. Rather, calcium fluxes, as indicated by the data, drive intracellular activation of calpain, and perhaps additional pathways. Results show that injury-induced elevations of calpain activity are inhibited by both calcium chelation and P188, and that P188 prevents injury-induced calcium increases. Thus, the data suggest that membrane poration drives increases in calcium levels and calcium-dependent calpain activity;

however, it cannot be currently ruled out that additional calpain regulatory mechanisms might also be involved. In addition, calcium is known to play a role in endogenous membrane repair mechanisms (McNeil and Steinhardt, 2003). Further studies are required to determine the exact mechanism by which P188 repairs the damaged plasma membrane and how it interacts with calcium-dependent repair processes.

It is not known whether activated calpain causes microtubule disruption. Calpain is known to degrade microtubule-associated proteins (MAPs) and monomeric tubulin (Billger et al., 1988); however, degredation of assembled microtubules has not been demonstrated. Axonal microtubules are known to undergo spontaneous depolymerization with high $[Ca^{2+}]_i$ levels (O'Brien et al., 1997) and to be severed by katanin (Ahmad et al., 1999) and spastin (Errico et al., 2002). It has been speculated that phosphorylation of MAPs could be regulating microtubule severing by blocking the access of katanins to microtubules (Baas and Qiang, 2005). Degradation of MAPs via injury-induced focal calpain activity might then eliminate this block and cause microtubule severing leading to the focal disruption of microtubule structure.

In this study mechanical trauma to primary central nervous system neurons was applied, and acute $[Ca^{2+}]_i$, and calpain responses were measured. Focal axonal beading, the hallmark morphology of DAI, was shown to be mediated by calcium-dependent calpain activity. $[Ca^{2+}]_i$ increase and calpain activity showed focal peaks along the axons which co-localized with mitochondria and predicted future axonal bead locations. P188, previously shown to block injury-induced microtubule disruption and axonal beading via resealing damaged membrane (Kilinc, et al., 2008), blocked the increase in $[Ca^{2+}]_i$ and calpain activity supporting the hypothesis that trauma induces Ca^{2+} influx through compromised cell membrane. These findings suggest that the restoration of membrane integrity is a valid therapeutic approach for acute intervention in TBI and that membrane damage is responsible for the ensuing calcium fluxes and calpain activation.

Acknowledgments

References

Ahmad FJ, Yu W, McNally FJ, Baas PW. An essential role for katanin in severing microtubules in the neuron. J Cell Biol 1999;145:305–15. [PubMed: 10209026]

Baas PW, Qiang L. Neuronal microtubules: when the MAP is the roadblock. Trends Cell Biol 2005;15:183–7. [PubMed: 15817373]

Billger M, Wallin M, Karlsson JO. Proteolysis of tubulin and microtubule-associated proteins 1 and 2 by calpain I and II. Difference in sensitivity of assembled and disassembled microtubules. Cell Calcium 1988;9:33–44. [PubMed: 2834062]

Blackman B, Barbee K, Thibault L. In vitro cell shearing device to investigate the dynamic response of cells in a controlled hydrodynamic environment. Annals of Biomedical Engineering 2000;28:363–372. [PubMed: 10870893]

Blumbergs PC, Scott G, Manavis J, Wainwright H, Simpson DA, McLean AJ. Topography of axonal injury as defined by amyloid precursor protein and the sector scoring method in mild and severe closed head injury. J Neurotrauma 1995;12:565–72. [PubMed: 8683607]

Borgens RB, Bohnert D, Duerstock B, Spomar D, Lee RC. Subcutaneous tri-block copolymer produces recovery from spinal cord injury. J Neurosci Res 2004;76:141–54. [PubMed: 15048938]

Buki A, Povlishock JT. All roads lead to disconnection?--Traumatic axonal injury revisited. Acta Neurochir (Wien) 2006;148:181–93. [PubMed: 16362181]discussion 193–4

Buki A, Siman R, Trojanowski JQ, Povlishock JT. The role of calpain-mediated spectrin proteolysis in traumatically induced axonal injury. J Neuropathol Exp Neurol 1999;58:365–75. [PubMed: 10218632]

Cadichon SB, Le Hoang M, Wright DA, Curry DJ, Kang U, Frim DM. Neuroprotective effect of the surfactant poloxamer 188 in a model of intracranial hemorrhage in rats. J Neurosurg 2007;106:36–40. [PubMed: 17233310]

Cargill RS 2nd, Thibault LE. Acute alterations in [Ca2+]i in NG108-15 cells subjected to high strain rate deformation and chemical hypoxia: an in vitro model for neural trauma. J Neurotrauma 1996;13:395–407. [PubMed: 8863195]

Coleman M. Axon degeneration mechanisms: commonality amid diversity. Nat Rev Neurosci 2005;6:889–98. [PubMed: 16224497]

Curry DJ, Wright DA, Lee RC, Kang UJ, Frim DM. Poloxamer 188 volumetrically decreases neuronal loss in the rat in a time-dependent manner. Neurosurgery 2004;55:943–8. [PubMed: 15458603] discussion 948–9

Detrait E, Eddleman CS, Yoo S, Fukuda M, Nguyen MP, Bittner GD, Fishman HM. Axolemmal repair requires proteins that mediate synaptic vesicle fusion. Journal of Neurobiology 2000;44:382–391. [PubMed: 10945894]

Errico A, Ballabio A, Rugarli EI. Spastin, the protein mutated in autosomal dominant hereditary spastic paraplegia, is involved in microtubule dynamics. Hum Mol Genet 2002;11:153–63. [PubMed: 11809724]

Farkas O, Lifshitz J, Povlishock JT. Mechanoporation induced by diffuse traumatic brain injury: An irreversible or reversible response to injury? J Neurosci 2006;26:3130–3140. [PubMed: 16554464]

Fineman I, Hovda DA, Smith M, Yoshino A, Becker DP. Concussive brain injury is associated with a prolonged accumulation of calcium: a 45Ca autoradiographic study. Brain Res 1993;624:94–102. [PubMed: 8252419]

Frim DM, Wright DA, Curry DJ, Cromie W, Lee R, Kang UJ. The surfactant poloxamer-188 protects against glutamate toxicity in the rat brain. Neuroreport 2004;15:171–4. [PubMed: 15106852]

Gaetz M. The neurophysiology of brain injury. Clinical Neurophysiology 2004;115:4–18. [PubMed: 14706464]

Geddes-Klein DM, Schiffman KB, Meaney DF. Mechanisms and consequences of neuronal stretch injury in vitro differ with the model of trauma. J Neurotrauma 2006a;23:193–204. [PubMed: 16503803]

Geddes-Klein DM, Serbest G, Mesfin MN, Cohen AS, Meaney DF. Pharmacologically induced calcium oscillations protect neurons from increases in cytosolic calcium after trauma. J Neurochem 2006b; 97:462–74. [PubMed: 16539664]

Gennarelli TA. The spectrum of traumatic axonal injury. Neuropathol Appl Neurobiol 1996;22:509–13. [PubMed: 9004238]

Gennarelli TA, Thibault LE, Graham DI. Diffuse Axonal Injury: An Important Form of Traumatic Brain Damage. Neuroscientist 1998;4:202–215.

Greenebaum B, Blossfield K, Hannig J, Carrillo CS, Beckett MA, Weichselbaum RR, Lee RC. Poloxamer 188 prevents acute necrosis of adult skeletal muscle cells following high-dose irradiation. Burns 2004;30:539–547. [PubMed: 15302418]

Iwata A, Stys PK, Wolf JA, Chen XH, Taylor AG, Meaney DF, Smith DH. Traumatic Axonal Injury Induces Proteolytic Cleavage of the Voltage-Gated Sodium Channels Modulated by Tetrodotoxin and Protease Inhibitors. J Neurosci 2004;24:4605–4613. [PubMed: 15140932]

Johnson GV, Litersky JM, Jope RS. Degradation of microtubule-associated protein 2 and brain spectrin by calpain: a comparative study. J Neurochem 1991;56:1630–8. [PubMed: 2013758]

Kampfl A, Posmantur R, Nixon R, Grynspan F, Zhao X, Liu SJ, Newcomb JK, Clifton GL, Hayes RL. mu-calpain activation and calpain-mediated cytoskeletal proteolysis following traumatic brain injury. J Neurochem 1996;67:1575–83. [PubMed: 8858942]

Kilinc D, Gallo G, Barbee KA. Mechanically-induced membrane poration causes axonal beading and localized cytoskeletal damage. Exp Neurol 2008;212:422–30. [PubMed: 18572167]

Kilinc D, Gallo G, Barbee KA. Interactive image analysis programs for quantifying injury-induced axonal beading and microtubule disruption. Comput Methods Programs Biomed 2009;95:62–71. [PubMed: 19285748]

LaPlaca MC V, Lee M, Thibault LE. An in vitro model of traumatic neuronal injury: loading rate-dependent changes in acute cytosolic calcium and lactate dehydrogenase release. J Neurotrauma 1997;14:355–68. [PubMed: 9219851]

Lee RC, River LP, Pan FS, Ji L, Wollmann RL. Surfactant-induced sealing of electropermeabilized skeletal muscle membranes in vivo. Proc Natl Acad Sci U S A 1992;89:4524–8. [PubMed: 1584787]

Liu J, Liu MC, Wang KK. Calpain in the CNS: from synaptic function to neurotoxicity. Sci Signal 2008;1:re1. [PubMed: 18398107]

Lusardi TA, Rangan J, Sun D, Smith DH, Meaney DF. A Device to Study the Initiation and Propagation of Calcium Transients in Cultured Neurons After Mechanical Stretch. Annals of Biomedical Engineering 2004;32:1546–1559. [PubMed: 15636114]

Maskarinec SA, Wu G, Lee KY. Membrane sealing by polymers. Ann N Y Acad Sci 2005;1066:310–20. [PubMed: 16533934]

Maxwell W, Watt C, Graham D, Gennarelli T. Ultrastructural evidence of axonal shearing as a result of lateral acceleration of the head in non-human primates. Acta Neuropathol 1993;86:136–144. [PubMed: 7692693]

Maxwell WL, Graham DI. Loss of axonal microtubules and neurofilaments after stretch-injury to guinea pig optic nerve fibers. J Neurotrauma 1997;14:603–14. [PubMed: 9337123]

Maxwell WL, McCreath BJ, Graham DI, Gennarelli TA. Cytochemical evidence for redistribution of membrane pump calcium-ATPase and ecto-Ca-ATPase activity, and calcium influx in myelinated nerve fibres of the optic nerve after stretch injury. J Neurocytol 1995;24:925–42. [PubMed: 8719820]

McCracken E, Hunter AJ, Patel S, Graham DI, Dewar D. Calpain activation and cytoskeletal protein breakdown in the corpus callosum of head-injured patients. J Neurotrauma 1999;16:749–61. [PubMed: 10521135]

McIntosh TK, Smith DH, Meaney DF, Kotapka MJ, Gennarelli TA, Graham DI. Neuropathological sequelae of traumatic brain injury: relationship to neurochemical and biomechanical mechanisms. Lab Invest 1996;74:315–42. [PubMed: 8780153]

McNeil PL, Steinhardt RA. Plasma membrane disruption: repair, prevention, adaptation. Annu Rev Cell Dev Biol 2003;19:697–731. [PubMed: 14570587]

Merenda A, Bullock R. Clinical treatments for mitochondrial dysfunctions after brain injury. Curr Opin Crit Care 2006;12:90–6. [PubMed: 16543782]

Merritt JE, McCarthy SA, Davies MP, Moores KE. Use of fluo-3 to measure cytosolic Ca2+ in platelets and neutrophils. Loading cells with the dye, calibration of traces, measurements in the presence of plasma, and buffering of cytosolic Ca2+ Biochem J 1990;269:513–9. [PubMed: 2117443]

O'Brien ET, Salmon ED, Erickson HP. How calcium causes microtubule depolymerization. Cell Motil Cytoskeleton 1997;36:125–35. [PubMed: 9015201]

Padanilam JT, Bischof JC, Lee RC, Cravalho EG, Tompkins RG, Yarmush ML, Toner M. Effectiveness of poloxamer 188 in arresting calcein leakage from thermally damaged isolated skeletal muscle cells. Ann N Y Acad Sci 1994;720:111–23. [PubMed: 7516633]

Raghupathi R. Cell death mechanisms following traumatic brain injury. Brain Pathol 2004;14:215–22. [PubMed: 15193035]

Robles E, Huttenlocher A, Gomez TM. Filopodial calcium transients regulate growth cone motility and guidance through local activation of calpain. Neuron 2003;38:597–609. [PubMed: 12765611]

Rosser BG, Powers SP, Gores GJ. Calpain activity increases in hepatocytes following addition of ATP. Demonstration by a novel fluorescent approach. J Biol Chem 1993;268:23593–600. [PubMed: 8226886]

Saatman KE, Abai B, Grosvenor A, Vorwerk CK, Smith DH, Meaney DF. Traumatic axonal injury results in biphasic calpain activation and retrograde transport impairment in mice. J Cereb Blood Flow Metab 2003;23:34–42. [PubMed: 12500089]

Saatman KE, Bozyczko-Coyne D, Marcy V, Siman R, McIntosh TK. Prolonged calpain-mediated spectrin breakdown occurs regionally following experimental brain injury in the rat. J Neuropathol Exp Neurol 1996;55:850–60. [PubMed: 8965100]

Schouten JW. Neuroprotection in traumatic brain injury: a complex struggle against the biology of nature. Curr Opin Crit Care 2007;13:134–42. [PubMed: 17327733]

Serbest G, Burkhardt MF, Siman R, Raghupathi R, Saatman KE. Temporal profiles of cytoskeletal protein loss following traumatic axonal injury in mice. Neurochem Res 2007;32:2006–14. [PubMed: 17401646]

Serbest G, Horwitz J, Barbee K. The effect of poloxamer-188 on neuronal cell recovery from mechanical injury. J Neurotrauma 2005;22:119–32. [PubMed: 15665607]

Serbest G, Horwitz J, Jost M, Barbee K. Mechanisms of cell death and neuroprotection by poloxamer 188 after mechanical trauma. FASEB J 2006;20:308–10. [PubMed: 16371428]

Servadei F, Compagnone C, Sahuquillo J. The role of surgery in traumatic brain injury. Curr Opin Crit Care 2007;13:163–8. [PubMed: 17327737]

Shapira Y, Yadid G, Cotev S, Shohami E. Accumulation of calcium in the brain following head trauma. Neurol Res 1989;11:169–72. [PubMed: 2573853]

Spaethling JM, Klein DM, Singh P, Meaney DF. Calcium-permeable AMPA receptors appear in cortical neurons after traumatic mechanical injury and contribute to neuronal fate. J Neurotrauma 2008;25:1207–16. [PubMed: 18986222]

Strich S. Shearing of Nerve Fibres as a Cause of Brain Damage due to Head Injury: A Pathological Study of Twenty Cases. The Lancet 1961;278:443–448.

Sun DA, Deshpande LS, Sombati S, Baranova A, Wilson MS, Hamm RJ, DeLorenzo RJ. Traumatic brain injury causes a long-lasting calcium (Ca2+)-plateau of elevated intracellular Ca levels and altered Ca2+ homeostatic mechanisms in hippocampal neurons surviving brain injury. Eur J Neurosci 2008;27:1659–72. [PubMed: 18371074]

Wang GJ, Jackson JG, Thayer SA. Altered distribution of mitochondria impairs calcium homeostasis in rat hippocampal neurons in culture. J Neurochem 2003;87:85–94. [PubMed: 12969255]

Wang KK, Larner SF, Robinson G, Hayes RL. Neuroprotection targets after traumatic brain injury. Curr Opin Neurol 2006;19:514–9. [PubMed: 17102687]

Wolf JA, Stys PK, Lusardi T, Meaney D, Smith DH. Traumatic Axonal Injury Induces Calcium Influx Modulated by Tetrodotoxin-Sensitive Sodium Channels. J Neurosci 2001;21:1923–1930. [PubMed: 11245677]

Xiong Y, Gu Q, Peterson PL, Muizelaar JP, Lee CP. Mitochondrial dysfunction and calcium perturbation induced by traumatic brain injury. J Neurotrauma 1997;14:23–34. [PubMed: 9048308]

Yoo S, Nguyen MP, Fukuda M, Bittner GD, Fishman HM. Plasmalemmal sealing of transected mammalian neurites is a gradual process mediated by Ca2+-regulated proteins. Journal of Neuroscience Research 2003;74:541–551. [PubMed: 14598298]

Zhou Z, Daugherty WP, Sun D, Levasseur JE, Altememi N, Hamm RJ, Rockswold GL, Bullock MR. Protection of mitochondrial function and improvement in cognitive recovery in rats treated with hyperbaric oxygen following lateral fluid-percussion injury. J Neurosurg 2007;106:687–94. [PubMed: 17432723]
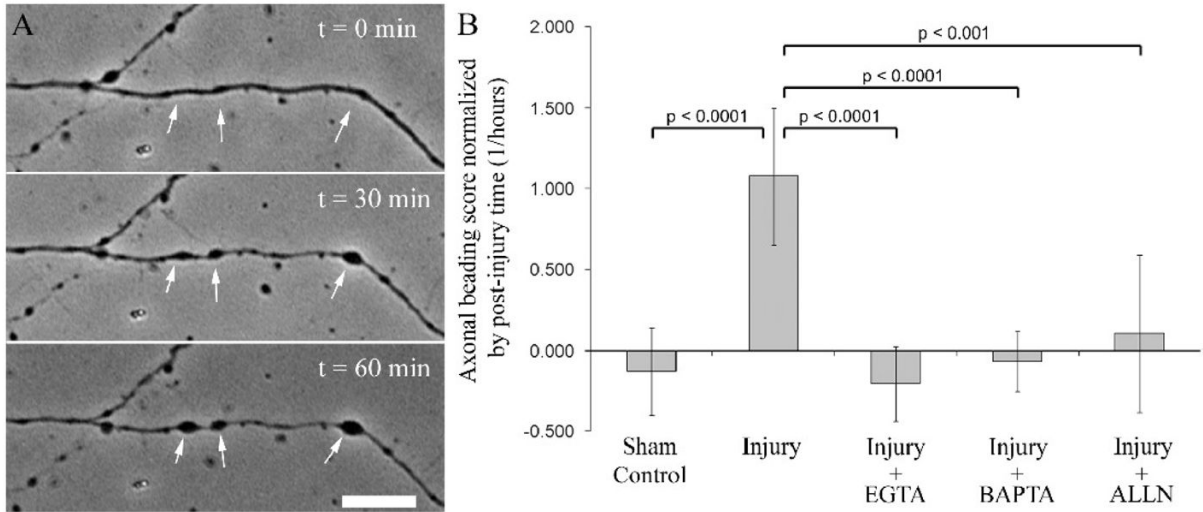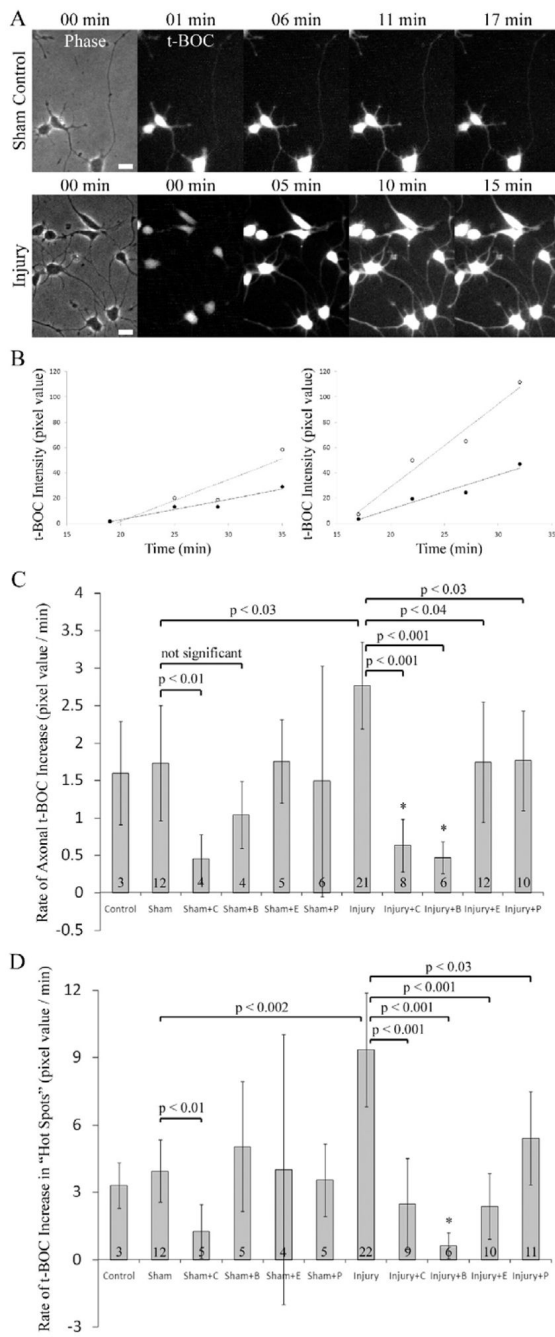
Figure 1.
Injury-induced axonal beading requires Ca^{2+}-dependent calpain activity. *A.* Axonal beading was observed following shear stress injury to the neurons (arrows). *B.* Change in the axonal beading score was normalized by post-injury period (hours). Injury-induced increase in the beading score is reduced to sham control levels when the shearing medium was buffered with 1mM EGTA, when the intracellular Ca^{2+} was chelated by 20μM BAPTA, or when the neurons were treated with 3μM calpain inhibitor ALLN prior to injury. ANOVA is followed by Tukey-Kramer test. Number of neurons analyzed is displayed on bars (Sham control: 18 neurons on 2 coverslips; injury: 54 neurons on 7 coverslips; injury + EGTA: 32 neurons on 4 coverslips; injury + BAPTA: 16 neurons on 2 coverslips; injury + ALLN: 22 neurons on 4 coverslips). Error bars represent 90% confidence intervals.
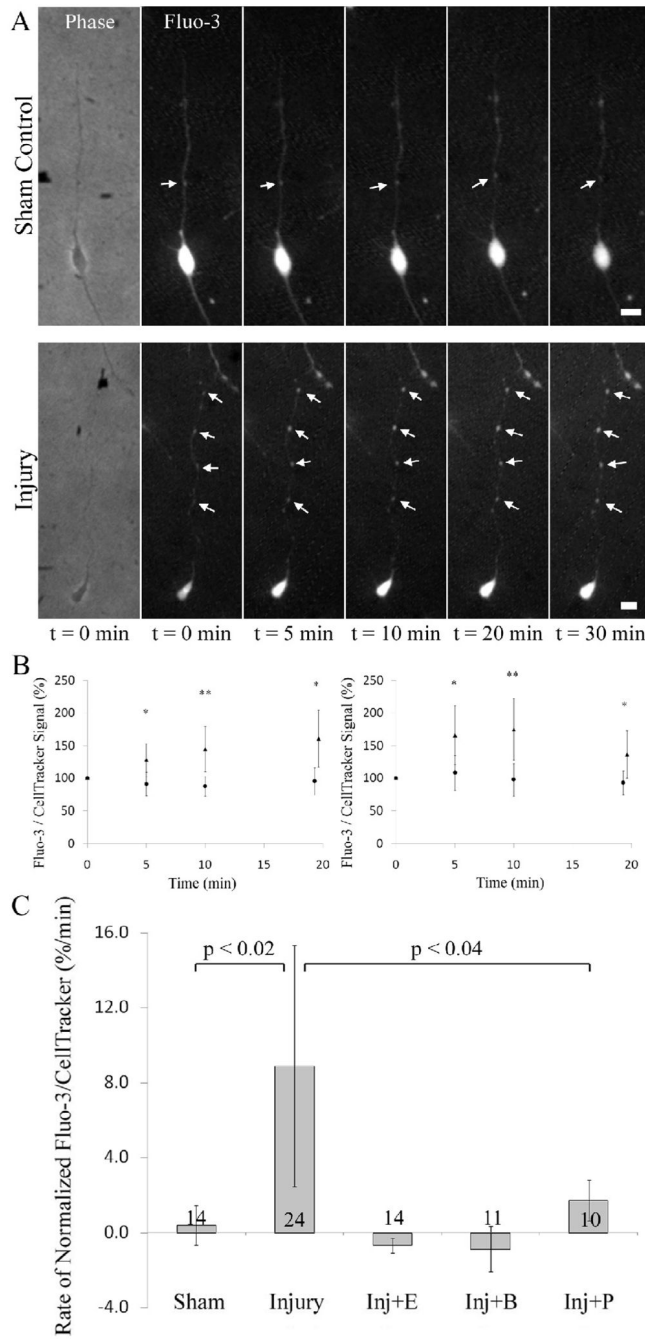
Figure 2.
Injury-induced increase in the intracellular calcium concentration. A. Both sham controls and injured neurons have focal $[Ca^{2+}]_i$ peaks. The signal intensity of the non-ratiometric Fluo-3 $[Ca^{2+}]_i$ indicator increases over time in the injured neuron compared to sham controls. B. In axonal areas (left panel) the intensity ratio of Fluo-3 signal over CellTracker Red signal increases steadily for the injury group (triangles, n = 24 neurons) compared to sham controls (circles, n = 14 neurons). At focal $[Ca^{2+}]_i$ peaks (right panel), the ratio for the injury group (triangles, 24 neurons) shows a sharp increase compared to sham controls (circles, n = 13 neurons) for the first 10 min but decreases to the axonal level during the rest of the post-injury period. * p < 0.05; ** p < 0.01. C. Mechanical injury induces an increase in the rate of change

of the normalized axonal $[Ca^{2+}]_i$ signal that can be blocked by EGTA, BAPTA and post-injury P188. ANOVA is followed by Tukey-Kramer test. Number of neurons analyzed is displayed on bars. Error bars represent 90% confidence intervals.

Figure 3.
Injury-induced increase in calpain activity. *A.* Signal intensity of t-BOC, a specific fluorescent substrate of calpain, increases significantly in the injured neurons compared to sham control. Time indicates the post-injury period. *B.* t-BOC intensity vs. time plots for the neurons shown in *A*. In sham controls, there is a gradual increase in the t-BOC signal indicating basal calpain activity. Both for the sham control (left graph) and the injured neuron (right graph) focal peaks (open circles) show a higher rate of increase than the axon average (filled circles). X-axes indicate time after t-BOC addition. *C.* and *D.* Calpain activity, measured by the rate of t-BOC signal intensity change, increases significantly in mechanically injured neurons and this increase is blocked by ALLN, BAPTA, EGTA, and post-injury P188 both in the axon and in

focal peaks. Control = Incubator controls; C = 3μM ALLN; B = 20μM BAPTA; E = 1mM EGTA; P = 100μM P188. ANOVA is followed by Tukey-Kramer test. *Significantly different from sham controls. Number of neurons analyzed is displayed on bars. Error bars represent 90% confidence intervals.
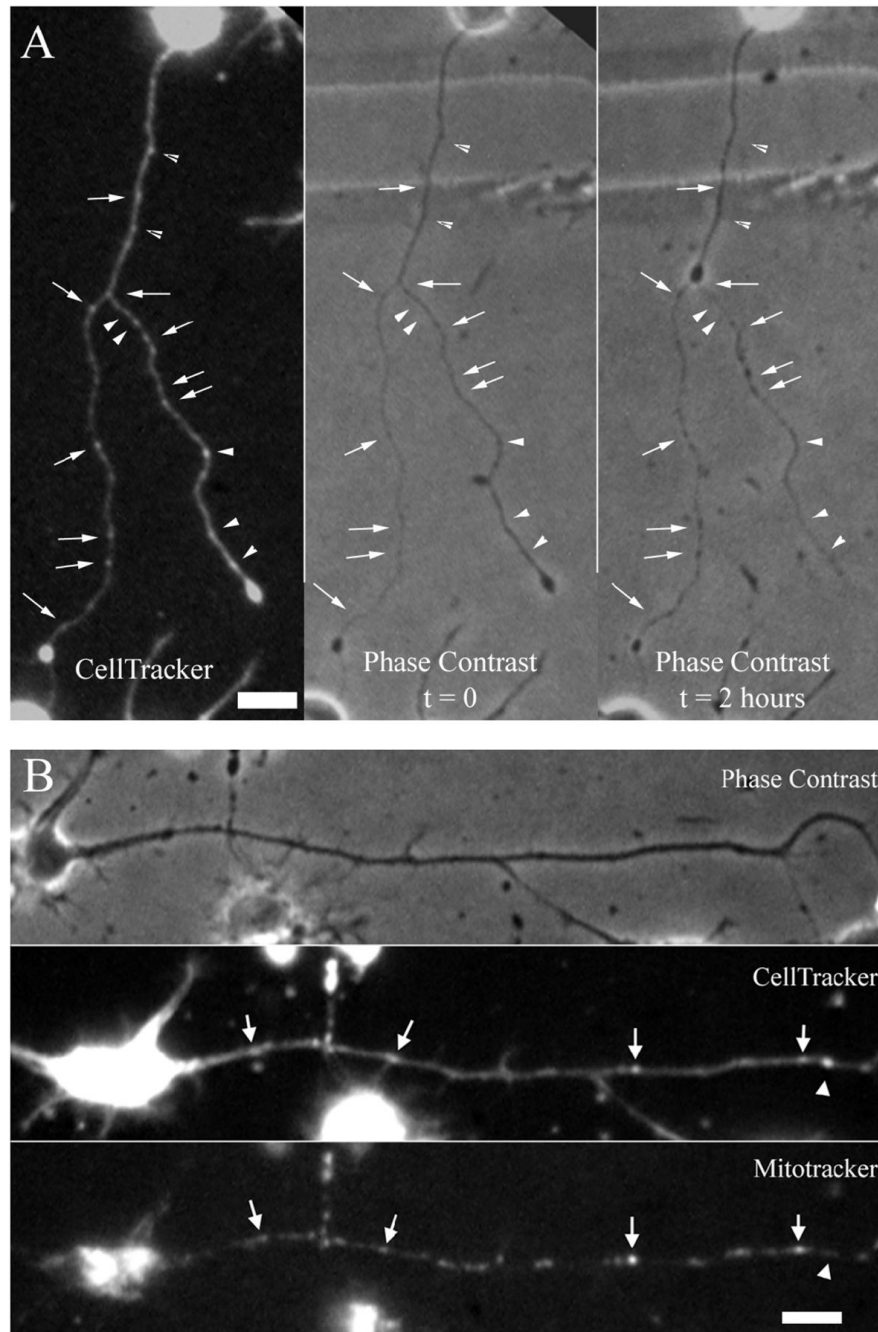
Figure 4.
Injury-induced axonal beads are associated with pre-injury densities of axonal mitochondria. *A,* Majority of focal CellTracker Red (CTR) concentration do not co-localize with morphological abnormalities before the injury. At 2 hours post-injury axonal beading is widespread and many bead locations co-localize with focal CTR peaks (arrows). However, not all focal peaks correspond to a bead location at this time point (arrowheads). *B,* Images of a control neuron double-stained with CTR and MitoTracker Green fluorescent markers. Focal peaks of the CTR image usually correspond to a high density area in the MitoTracker image (arrows). However, some focal peaks do not correspond to any mitochondrion (arrowhead).

Phase contrast image of the same control neuron reveals that focal CTR peaks may naturally exist in an axon without any beading morphology. Bars = 10μm.